Redox Biology 14 (2018) 198–210

Contents lists available at ScienceDirect

Redox Biology

journal homepage: www.elsevier.com/locate/redox

Integrated metabolic models for xenobiotic induced mitochondrial toxicity in skeletal muscle

William Dott[a], Jayne Wright[b], Kelvin Cain[c], Pratibha Mistry[b], Karl E. Herbert[a,*]

[a] Department of Cardiovascular Sciences, University of Leicester, UK
[b] Syngenta Ltd., Jealott's Hill, UK
[c] MRC Toxicology Unit, University of Leicester, Leicester, UK

ABSTRACT

There is a need for robust *in vitro* models to sensitively capture skeletal muscle adverse toxicities early in the research and development of novel xenobiotics. To this end, an *in vitro* rat skeletal muscle model (L6) was used to study the translation of transcriptomics data generated from an *in vivo* rat model. Novel sulfonyl isoxazoline herbicides were associated with skeletal muscle toxicity in an *in vivo* rat model. Gene expression pathway analysis on skeletal muscle tissues taken from *in vivo* repeat dose studies identified enriched pathways associated with mitochondrial dysfunction, oxidative stress, energy metabolism, protein regulation and cell cycle. Mitochondrial dysfunction and oxidative stress were further explored using *in vitro* L6 metabolic models. These models demonstrated that the sulfonyl isoxazoline compounds induced mitochondrial dysfunction, mitochondrial superoxide production and apoptosis. These *in vitro* findings accurately concurred with the *in vivo* transcriptomics data, thereby confirming the ability of the L6 skeletal muscle models to identify relevant *in vivo* mechanisms of xenobiotic-induced toxicity. Moreover, these results highlight the sensitivity of the L6 galactose media model to study mitochondrial perturbation associated with skeletal muscle toxicity; this model may be utilised to rank the potency of novel xenobiotics upon further validation.

1. Introduction

In vitro cell models can provide a surrogate system for *in vivo* experimentation particularly where cell culture conditions are customised to influence the physiology of the cell system. Here we utilise a rat skeletal muscle cell line, L6, previously studied in galactose media for optimal assessment of mitochondrial perturbation [1] to study pathways identified from *in vivo* gene expression analysis. Culture in galactose sensitizes cells to agents that cause mitochondrial toxicity [2]. In response to mitochondrial toxicity, cells grown in glucose-containing media engage the 'Crabtree effect' and are able to switch to glycolysis to generate ATP, thereby mitigating the severe metabolic effects of mitochondrial compromise. The sensitization observed in cells cultured in galactose is in part due to an inability to utilise the Crabtree effect; metabolism of galactose is inefficient and cells rely upon supplied glutamine entering the tricarboxylic acid cycle to generate ATP. *In vitro* cell culture models have been suggested for screening for mitochondrial liabilities early in the development of drugs and agrochemicals [3] and is particularly relevant for chemicals that might act *via* cardio- or skeletal muscle toxicity, where mitochondrial ATP generation is a key process.

Transcriptomics has been successfully applied to identify toxicant-induced perturbations of cellular pathways [4,5]. A number of studies have compared *in vitro* and *in vivo* xenobiotic-induced genomic responses [6–9]. These studies conclude that comparison at the pathway level is more effective than at the single gene level. For example, Boess et al. [8] showed that the *in vivo* hepatotoxic potential of two compounds could be assessed *in vitro* using biochemical endpoints and/or transcriptomics.

Skeletal muscle toxicity has become an area of interest given the propensity of xenobiotics to induce such toxicities. In the pharmaceutical industry, the potential for skeletal muscle toxicity was highlighted by the withdrawal of Cerivastatin in 2001 due to rhabdomyolysis, a potentially fatal deleterious injury to skeletal muscle [10]. Consequently, the validation of *in vitro* skeletal muscle models may play a role in assessing the safety profile of industrial compounds.

Novel sulfonyl isoxazoline herbicides were associated with cardiac and/or skeletal muscle toxicity. Guided by transcriptomics, this study evaluated the translation of rat *in vivo* toxicity findings to an *in vitro* skeletal muscle cell model. Gene expression pathway analysis was

* Correspondence to: Department of Cardiovascular Sciences, University of Leicester, Glenfield Hospital, Leicester LE3 9QP, UK.
E-mail address: keh3@le.ac.uk (K.E. Herbert).

http://dx.doi.org/10.1016/j.redox.2017.09.006
Received 10 May 2017; Received in revised form 11 September 2017; Accepted 13 September 2017
Available online 18 September 2017

conducted on skeletal muscle tissue taken from animals treated at sub-toxic doses in a 28 day repeat dose study. The pathways hypothesised to be associated with sulfonyl isoxazoline compound toxicity were then investigated in the L6 skeletal muscle model, using a range of relevant biochemical endpoints.

2. Materials and methods

2.1. Materials

All chemicals were supplied by Sigma-Aldrich unless otherwise stated. MitoSox™, MitoTracker® Red, DHE, CMXRos and ATP determination kit were purchased from Molecular Probes Inc., Life Technologies UK Ltd. All materials and reagents for the Extracellular Flux assays were from Agilent Seahorse (Santa Clara, CA). Novel research sulfonyl isoxazoline herbicide chemistries were supplied by Syngenta (Syngenta Ltd., Jealott's Hill, Berkshire, UK). The sulfonyl isoxazoline compounds were designed to inhibit the biosynthesis of very-long-chain fatty acids in plants. Two sulfonyl isoxazoline compounds were studied, referred to as compounds 177 and 197, which differ by the position of a halogenated triazole substitution on the core sulfonyl isoxazoline. For all *in vitro* experiments, cells were exposed to sulfonyl isoxazoline compounds (to maximum solubilities) in a final of concentration of 1% DMSO.

2.2. Animal studies

The rat studies were conducted at Charles River Laboratory (CRL), UK and based on OECD guidelines No. 407, July 27, 1995. Throughout the studies, rats had access to domestic water and diet (Rat and Mouse modified No. 1 Diet SQC Expanded (Ground) supplied by Special Diets Services Limited, 1 Stepfield, Witham, Essex) *ad libitum*. 4 week old female Han Wistar rats (n = 5/ dose) were acclimatised for a minimum of 2 weeks prior to continuous treatment *via* the diet for 28 days. The treatment concentration was achieved by mixing the test compound into the diet (as indicated by parts per million-ppm. One ppm being equivalent to 1 mg sulfonyl isoxazoline per kg diet). The quantity of food consumed by each cage of animals was measured and recorded twice during pre-study, daily during the first week of treatment, then twice weekly thereafter until the completion of treatment. The amount of experimental diet ingested was calculated at regular intervals during treatment using the following formula:

$$\text{Achieved intake(mg/kg body weight/day)} = \frac{\text{Concentration(ppm)} \times \text{Food Consumption(g/day)}}{\text{Mid} - \text{point Body Weight*}}$$

*an average of the body weights at the start and end of each period for which food consumption was measured. The achieved dosages are summarised in Table 1.

2.3. Animal monitoring

Animals were checked twice daily for viability and detailed clinical examination was conducted weekly, including appearance, movement and behaviour patterns, skin and hair condition, eyes and mucous membranes, respiration and excreta. Body weights and food consumption were monitored prior to and throughout the treatment as appropriate and recorded.

Table 1
Dietary intake of sulfonyl isoxazoline compounds in 28 day repeat dose studies in female rats.

sulfonyl isoxazoline compound	Dose	Dietary Intake for Oral diet
177	0, 5, 30 & 150 ppm	0, 0.58, 3.35 and 16.89 mg/kg/D (n = 5 in ♀)
197	0, 150, 1500 & 5000 ppm	0, 16, 156, 549 mg/kg/D (n = 5 in ♀)

2.4. Necropsy and histopathology

After 28 days of treatment rats were killed in a randomized order by exposure to carbon dioxide and terminal body weights were recorded followed by exsanguination. Animals were necropsied and descriptions of all macroscopic abnormalities were recorded. Organs were removed and weighed before preservation in 10% neutral buffered formalin and processed to paraffin. Sections of 4–6 μm were stained with haematoxylin and eosin (H & E) and examined by light microscopy. Note, skeletal muscle histopathology assessments were conducted on the diaphragm and soleus muscle; and the femoris muscle preserved for gene expression analysis.

2.5. Clinical pathology

Blood samples for routine haematology, coagulation and clinical chemistry were obtained *via* the orbital sinus under isoflurane anaesthesia prior to termination. Whole blood was transferred into tubes containing EDTA for haematology investigations, lithium heparin tubes for clinical chemistry investigations and processed for serum for cardiac biomarker analysis. The samples were analysed according to standard CRL laboratory protocols for; haematology using Bayer, ADVIA 120 haematology analyser and clinical chemistry using Roche P module Clinical chemistry Analyser with Roche test kit.

2.6. RNA extraction

An RNeasy fibrous kit (Qiagen, Manchester, UK) was used to extract total RNA from femoris (thigh) skeletal muscle (TSM) tissue samples. Briefly, approximately 20–25 mg of each tissue sample was pulverized using a mortar and pestle and following the addition of lysis buffer (RLT) they were homogenised using a rotor-stator homogeniser (8 mm tip). The remainder of the extraction was carried out according to the manufacturer's instructions and included the optional DNase kit (Qiagen, Manchester, UK) to remove contaminating DNA. RNA quantity and purity was determined using an ND-1000 UV Spectrophotometer (NanoDrop technologies) and the quality was assessed with the Agilent 2100 Bioanalyzer (Agilent). RNA samples used in this study all had a 260/280 and 260/230 ratio in the range 1.8–2.07 and 1.8–2.2, respectively, and an RNA Integrity Number (RIN) above 7.0.

2.7. Microarray gene expression analysis

2.7.1. cRNA amplfication and labelling

The Illumina TotalPrep RNA amplification kit (Ambion, UK) was used for cRNA amplification and labelling as detailed in the manufacturer's instructions. cRNA quantity and purity was assessed using an ND-1000 UV Spectrophotometer and quality was assessed with the Agilent 2100 Bioanalyzer. cRNA samples used in this study had the same purity as described above for RNA and a size distribution between 1000 and 1500 nt.

2.8. Hybridization, staining and scanning

The equipment, materials and reagents used to hybridize the cRNA are detailed in the 'Whole Genome Gene Expression Direct Hybridization Assay guide' (Illumina) and supplied by Illumina unless otherwise stated. As detailed in the manufacturer's instructions, biotin-labelled cRNA (750 ng in 5 μl) samples were hybridized to the RatRef-12 whole genome gene expression BeadChips, developed by Illumina. This BeadChip allowed for the analysis of 22,519 probes per sample,

targeting 21,910 genes selected primarily from the NCBI RefSeq database and processed 12 samples per chip. Following hybridization, the BeadChips were washed and stained using streptavidin-Cy3 (Sigma-Aldrich, Dorset, UK), according to manufacturer's instructions. After staining, the BeadChips were scanned on an Illumina BeadArray Reader with Bead scan software (Illumina).

2.9. Microarray data analysis

Following the BeadChip scan, GenomeStudio software (Illumina) was used to produce bead summary data from the raw data, which was exported as a custom report using the 'ArrayExpress Data submission Report plug-in V2.0.0'. The average probe signal (on the unlogged scale), probe ID and detection P value were imported into ArrayTrack, a software system developed by the FDA for the management, analysis, visualisation and interpretation of microarray data [11]. Within ArrayTrack normalisation, correlation analysis, cluster analysis and differential gene expression analysis were carried out. First, the raw data was log (base 2) transformed and quantile normalisation without background subtraction was carried out; a normalisation method recommended in previous studies [12,13]. The data presented here are deposited in the NCBI Gene Expression Omnibus [14] accessible through GEO Series accession number GSE GSE101847 (https://www.ncbi.nlm.nih.gov/geo/query/acc.cgi?acc=GSE101847).

To assess the quality and reproducibility of the microarrays and identify outliers, Pearson's correlation coefficient of pair-wise Log2 intensity correlation was calculated, using the Correlation matrix tool in ArrayTrack. The entire normalised data set was used (a total of 22,519 probes), without a specific cut-off. Samples from the same tissue origin were analysed together and arrays were considered highly reproducible > 0.9 and any samples < 0.8 were discarded from further analysis. Two forms of clustering analysis, principal component analysis (PCA) and hierarchical clustering analysis (HCA) were used to analyse the normalised data set, without a specific cut off. To identify differentially expressed genes, a Student's *t*-test was carried between the normalised control and treated sample expression lists. To account for multiple testing, P-values were adjusted using Benjamani and Hochberg's false discovery rate (FDR) [15]. Differences in relative expression were considered significant at an FDR-adjusted $P < 0.05$, but if the FDR was too strict, an unadjusted P-value of < 0.05 was used. An unadjusted P-value was considered acceptable in the current study since most scientists are willing to accept some errors will occur in microarray and the more generous statistical power of functional analysis can reveal significant changes that are not apparent at the single gene level, providing hypotheses for follow up analysis [16–19].

2.10. Functional analysis of DEG

Functional analysis was performed using Ingenuity Pathway analysis (IPA; Ingenuity® Systems, Redwood City, CA, USA) (www.ingenuity.com) and Database for Annotation and Visualisation and Integrated Discovery (DAVID) [20]. Lists of DEGs, containing GeneBank accession IDs, fold changes and p values were uploaded into IPA. The IPA 'Core Analysis' function was used to interpret the data in the context of; biological and toxicity functions, canonical pathways, toxicity lists and networks. Right-tailed Fisher's exact test was applied to determine the level of significance for each network, pathway and list and the p-value was displayed as a score, which is the negative log of that p-value. For canonical pathways and ToxLists, a score of > 1.3, which equates to a $P < 0.05$, was considered significant. Only networks with a score of > 3, $P < 0.001$, were considered significant. The same gene lists as for IPA were uploaded into DAVID using GenBank Accession ID, and the entire annotated Illumina RatRef array was used as background. Analysis was performed using the default functional tools of DAVID following the criteria suggested [20]. Results with an EASE score of < 0.1 were considered, unless terms were enriched with a Benjamani-Hochberg multiple correction test, in which case an adjusted P-value < 0.05 was used as the cut-off. Functional Annotation Clustering and gene functional classification tools were used with the > medium classification stringency in order to group redundant terms and determine their overall enrichment score. For clustering, an enrichment score of > 1.3 (equivalent to $P < 0.05$) was considered in the analysis.

2.11. Cell culture conditions

2.11.1. High glucose media

The high-glucose media consisted of Dulbecco's modified Eagle's medium (DMEM) (Invitrogen), containing 25 mM glucose and 1 mM sodium pyruvate and supplemented with 5 mM N-2-hydroxyethylpiperazine-N'-2-ethanesulfonic acid (HEPES), 10% FBS, penicillin (100IU/ml) and streptomycin (100 μg/ml).

2.11.2. Galactose media

The galactose media consisted of DMEM without glucose (Invitrogen) supplemented with 10 mM galactose, 2 mM glutamine (6 mM final), 5 mM HEPES, 10% FBS, 1 mM sodium pyruvate, and penicillin/streptomycin as above.

L6 cells are a myoblast cell line derived from rat femoris muscle (ATCC). These were grown in either of glucose or galactose-containing media for a minimum of 7 days before experimentation. To evaluate if the cells had adapted to galactose media, they were treated with antimycin A (AMA) and toxicity was compared with the toxicity observed in glucose media.

2.12. Measurement of cell viability & ATP content

The sensitive colorimetric cell counting kit assay (CCK-8) was used to assess cell viability according to the manufacturer's protocol and measured at 450 nm using a BioTek Elx800 microplate reader (BioTek UK). Cellular ATP concentrations were assessed using the ATP Determination kit as instructed in the manufacturer's protocol and a NOVOstar luminometer.

2.13. Analysis of mitochondrial function in L6 cells

Measurements of L6 cell oxygen consumption rate (OCR) and extracellular acidification rate (ECAR) were made using the Seahorse XF24 Analyzer (Agilent, CA) as described previously [1]. As described in [1], mitochondrial function was analysed by sequential addition of pharmacological inhibitors of oxidative phosphorylation. The resultant bioenergetic profile provides detailed information on the individual components of the respiratory chain. For a detailed and extensive review on the interpretation of the bioenergetic profile, please refer to [21]. Briefly, six parameters of mitochondrial function were calculated from the bioenergetic profile: basal OCR, ATP-linked OCR, proton leak OCR, maximal OCR, reserve capacity and non-mitochondrial OC.

2.14. Detection of mitochondrial and cytosolic superoxide

Intracellular cytosolic and mitochondrial-derived superoxide production was measured on a CyAn ADP flow cytometer using dihydroethidium (DHE) and MitoSOX™ red, respectively, as detailed according to the manufacturer's protocol.

2.15. Measurement of apoptosis

To characterise apoptosis and necrosis, cells were stained using the Annexin V-FITC Apoptosis Kit (Abcam, Cambridge, UK) and analysed using a CyAn ADP flow cytometer and using the Summit V4.3.02 software. The activity of caspases 3 and 7 were quantified using the luminescent assay Caspase-Glo® 3/7 assay (Promega, Southampton, UK) and a NOVOstar luminometer at 24 °C.

2.16. Statistical analysis

All data are presented as mean and standard error of the mean (SEM) or standard deviation (SD) as appropriate. Statistical analyses were performed using Graphpad Prism® 6 software (GraphPad Software, Inc., La Jolla, CA, USA). Statistical significance of the data was assessed by paired student's *t*-test, one-way Analysis of Variance (ANOVA) (with Dunnett's multiple comparison test) or two-way ANOVA (with Sidak's or Tukey's multiple comparison test) as appropriate. A P-value of < 0.05 was considered statistically significant. IC50 values were calculated in Graphpad Prism using a nonlinear regression curve fit with 4 parameters. The maximum (DMSO control) and minimum values (total cell kill) were fixed.

3. Results

3.1. In-life study observations

There were no premature decedents during the study or clinical signs that could be attributed to treatment. There were no other differences in body weight or food and water consumption that were considered to be related to treatment, except for a transient palatability effect in rats dosed daily with 5000 ppm compound 197 in the first 11 days.

3.2. Terminal study observations

There were no treatment related necropsy findings and there were no significant changes in haematological or coagulation parameters attributed to treatment. Dietary administration of compound 197 at 5000 ppm was associated with squamous cell hyperplasia and hyperkeratosis in the non-glandular stomach, hepatocyte degeneration and hypertrophy in the liver, myocardial degeneration in the heart and myofibre degeneration in the skeletal muscles (Fig. 1). Myofibre degeneration was used to describe scattered abnormal myocytes characterised either by swollen hypereosinophilic cytoplasm with central pallor, or by central cytoplasmic degeneration with a granular eosinophilic border. There were also associated increases in liver weight in this dose group and a number of clinical chemistry parameters (namely, alanine aminotransferase, aspartate aminotransferase, gamma glutamyl transferease, total bilirubin, cholesterol levels and triglycerides). Dietary administration of compound 177 at 150 ppm and 197 at 150 and 1500 ppm resulted in myofibre degeneration of the diaphragm and myositis of the soleus muscle. In addition, myositis of the soleus muscle was also seen in animals treated with compound 177 at 30 ppm, and minimal cardiac injury in animals treated with compound 197 at 150 and 1500 ppm. All other changes in the treatment groups for both compounds were considered incidental and typical for the strain of rat.

3.3. In vivo transcriptomics results

Gene expression profiles of TSM from female rats treated for 28 days with 150 ppm of sulfonyl isoxazoline compounds were determined. There were four biological replicates for control and treated groups. Clustering analysis (PCA and HCA) identified a clear separation between control and treated samples for compound 197, demonstrating that compound 197 had a distinct effect on TSM gene expression after 28 days (Fig. S1). The clustering of control and treated samples was not as distinct with compound 177; HCA was unable to cluster control and treated samples for this compound (Fig. S1). Differentially expressed genes (DEG) between control and treated samples were calculated using a T-test and DEG were selected using a significance cut-off of FDR ≤ 0.05 for 197 and a $P \leq 0.05$ for compound 177.

3.4. Functional analysis of differentially expressed genes

Functional analysis was carried out with IPA and DAVID on TSM from rats exposed to compound 177 and 197 [22]. Table 2 shows the IPA toxicity lists and canonical pathways and Table 3 lists the KEGG pathways most significantly enriched in TSM following treatment with 177 and 197. There was considerable overlap of biological processes significantly enriched by both compounds, suggesting a common sulfonyl isoxazoline mechanism of toxicity. These commonly enriched biological processes were associated with mitochondrial dysfunction, oxidative stress, energy metabolism, cell death and survival signaling, protein regulation and cell cycle/DNA damage response.

Biological processes relating to mitochondrial dysfunction and oxidative stress were the most commonly and significantly enriched by both compounds. Most notably, the toxicity list '*mitochondrial dysfunction*' was highly significantly enriched by both compounds. The enrichment of KEGG pathways '*oxidative phosphorylation*' by both compounds and *'ubiquinone and other terpenoid-quinone biosynthesis'* by 177 provided further evidence of mitochondrial perturbation.

The enrichment of the toxicity lists *'oxidative stress'* and '*NRF2-mediated Oxidative Stress Response*' by 197 and a number of antioxidant canonical pathways by 177 (including '*Arsenate Detoxification I (Glutaredoxin),*' '*Thioredoxin pathway', 'Antioxidant action of vitamin C and Ascorbate recycling'*) provided significant evidence for induction of oxidative stress by these compounds. The enrichment of '*RAR activation'* by 197 is indicative of a significant transcriptional activation in response to oxidative stress. Activation of this pathway has been shown to prevent apoptosis in adult cardiomyocytes following high-glucose-induced oxidative stress [23]. The enrichment of KEGG pathways related to neurological diseases (Alzheimer's, Parkinson's and Huntington's) by both compounds was also significant, since the pathogenesis of these diseases has been strongly linked to oxidative stress and mitochondrial dysfunction [24,25].

Consistent with effects on mitochondria, there was a profound enrichment of pathways relating to energy metabolism with both sulfonyl isoxazoline compounds. IPA analysis highlighted the prominent role of PPAR signaling in response to sulfonyl isoxazoline treatment. The toxicity list '*Mechanism of gene regulation by PPARα'* was highly significantly enriched by both compounds and the toxicity list '*PPARα/RXRα Activation'* and canonical pathway *'PPAR signaling'* was significantly enriched by 197 and 177, respectively. The activation of PPARα is notable since it is a key player in the transcriptional regulation of mitochondrial biogenesis following mitochondrial damage. KEGG pathway analysis also supported effects on energy metabolism following treatment with 197 with the enrichment of '*fatty acid metabolism', 'glycolysis/ Gluconeogenesis', 'fatty acid β-oxidation'*. The enrichment of these energy metabolism pathways is indicative of effects on mitochondria, given the fact that mitochondria provide most of the energy necessary for cell homeostasis,

There were a number of cell cycle and DNA damage related pathways and toxicity lists enriched by both compounds, which provided strong evidence for the involvement of oxidative stress in response to sulfonyl isoxazoline treatment. The canonical pathway '*cell cycle regulation by BTG family proteins'* was significantly enriched by 177, which is a protein family that has been implicated in the G2/M DNA damage checkpoint [26]. Similarly, the toxicity list '*cell cycle: G2/M DNA damage checkpoint regulation'* was significantly enriched by 197. Moreover, the KEGG pathway *'nucleotide excision repair'* was significantly enriched by 197, which is the most important repair system to remove DNA lesions caused by ROS.

Finally, a number of pathways significantly enriched by 197 related to stress response signaling, including '*HIF signaling', 'PTEN signaling', 'Regulation of eiF4 and p70S6k signaling'* and '*eiF2 signaling*'. Of these pathways, eiF4 and p70S6K plays an important role in a number of processes, including autophagy, lipid synthesis, mitochondrial metabolism and mitochondrial biogenesis [27].

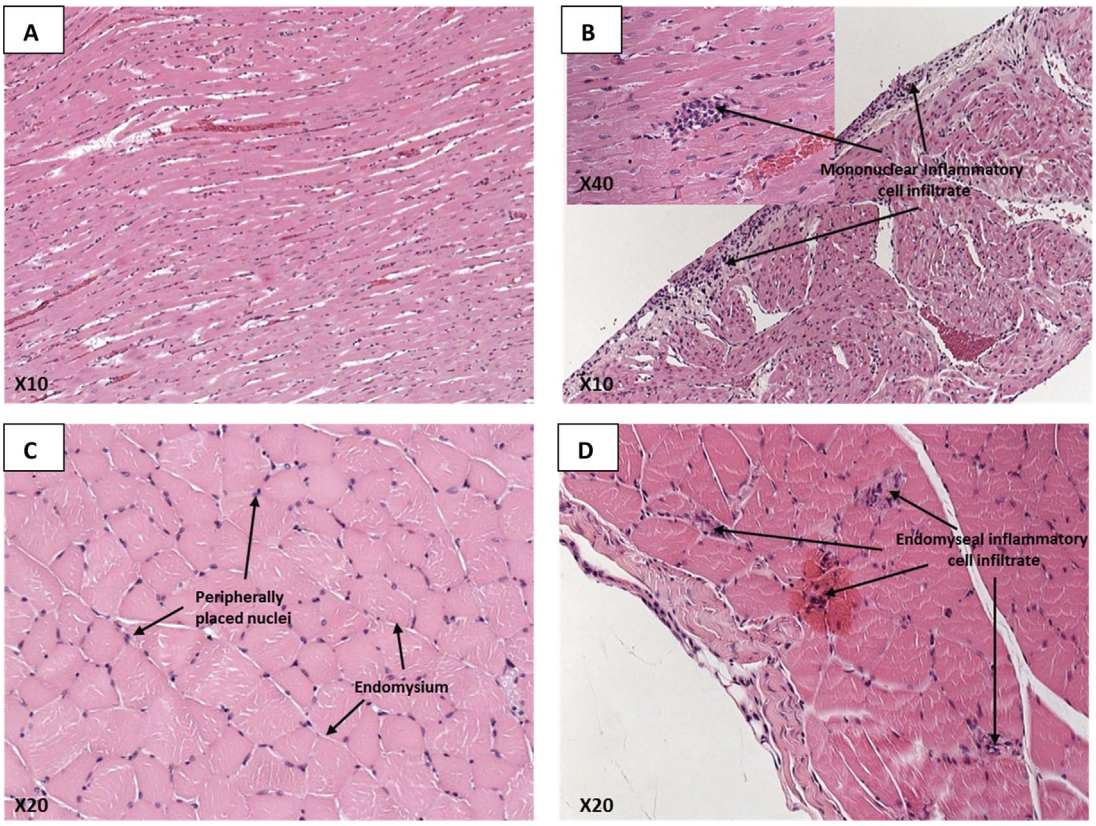

Fig. 1. Representative histopathological images of skeletal and cardiac muscle tissue sections from female Han Wistar rats showing changes typical of the effects of sulfonyl isoxazoline compounds in 28 day dietary studies. Panels A and B are cardiac muscle sections from rats treated with control diet (A) and compound 177 (B). Panel C and D are skeletal muscle sections from rats treated with control diet (C) and diet with compound 197 for 28 days (D). Samples are 10% neutral buffered formalin-fixed paraffin-embedded tissue Sections (4–6 μm) stained with haematoxylin and eosin.

Table 2
IPA analysis of 197 and 177 TSM.

197 TSM			
Toxicity Lists	**-log (P-V)**	**Canonical Pathways**	**-Log (P-V)**
RAR Activation	4.21	Protein Ubiquitination Pathway	13.7
Hypoxia-Inducible Factor (HIF) Signaling	3.60	eiF2 Signaling	10.8
Mechanism of Gene Regulation by Peroxisome Proliferators *via* PPARα	2.36	tRNA Charging	5.52
Mitochondrial Dysfunction	2.03	Regulation of eIF4 and p70S6K Signaling	5.13
Cholesterol Biosynthesis	1.68	Estrogen Receptor Signaling	4.79
PPARα/RXRα Activation	1.67	RAR Activation	4.32
Cell Cycle: G2/M DNA Damage Checkpoint Regulation	1.65	PTEN Signaling	4.05
Oxidative Stress	1.47	Hypoxia Signaling in the Cardiovascular System	3.52
NRF2-mediated Oxidative Stress Response	1.34	IGF-1 Signaling	3.00
TGF-β Signaling	1.19	Mitotic Roles of Polo-Like Kinase	2.88
177 TSM			
Toxicity Lists	**-log (P-V)**	**Canonical Pathways**	**-log (P-V)**
Mitochondrial Dysfunction	2.76	Mitochondrial Dysfunction	2.81
Mechanism of Gene Regulation by Peroxisome Proliferators *via* PPARα	1.30	Ascorbate Recycling (Cytosolic)	2.64
Increases Depolarization of Mitochondria and Mitochondrial Membrane	1.09	Arsenate Detoxification I (Glutaredoxin)	2.34
Glutathione Depletion - Phase II Reactions	0.97	Antioxidant Action of Vitamin C	2.29
Decreases Permeability Transition of Mitochondria and Mitochondrial Membrane	0.87	Thioredoxin Pathway	1.96
LPS/IL-1 Mediated Inhibition of RXR Function	0.81	Valine Degradation I	1.88
VDR/RXR Activation	0.75	Cell Cycle Regulation by BTG Family Proteins	1.79
Cytochrome P450 Panel - Substrate is a Vitamin (Mouse)	0.74	PPAR Signaling	1.79
Cytochrome P450 Panel - Substrate is a Vitamin (Rat)	0.74	2-amino-3-carboxymuconate Semialdehyde Degradation to Glutaryl-CoA	1.55
Oxidative Stress	0.66	Tumoricidal Function of Hepatic Natural Killer Cells	1.54

The top 10 enriched toxicity lists and canonical pathways of 177 TSM DEG ($P < 0.05$) and 197 TSM DEG (FDR < 0.05) are listed. log (P-V) = $-\log_{10}$ (P-value), which is known as a P-score. A P score of ≥1.3 was considered significant, which equates to a p value of < 0.05.

Table 3
KEGG pathway analysis of 197 and 177 TSM.

177 TSM KEGG Terms	P-Value	197 TSM KEGG Terms	P-Value
Oxidative phosphorylation	5.5E−04	Ribosome	8.75E−23
Alzheimer's disease	5.3E−03	Spliceosome	4.46E−07
Parkinson's disease	7.4E−03	Proteasome	4.91E−06
Huntington's disease	1.6E−02	RNA degradation	1.14E−05
Proteasome	1.8E−02	Ubiquitin mediated proteolysis	2.74E−05
Ubiquinone and other terpenoid-quinone biosynthesis	2.4E−02	Aminoacyl-tRNA biosynthesis	2.44E−04
		Cell cycle	8.88E−04
		Oxidative phosphorylation	0.00344
		Huntington's disease	0.00469
		Parkinson's disease	0.00589
		Basal transcription factors	0.00778
		Alzheimer's disease	0.0144
		Glycolysis / Gluconeogenesis	0.01677
		Nucleotide excision repair	0.03974
		TGF-beta signaling pathway	0.04065
		Other glycan degradation	0.04317
		SNARE interactions in vesicular transport	0.04479

The significant KEGG pathways ($P < 0.05$) for 197 TSM DEG (FDR < 0.05) and 177 TSM DEG ($P < 0.05$) are listed.

3.5. Effects of sulfonyl isoxazoline compounds on cell viability and cell death

To investigate whether the biological processes identified using *in vivo* transcriptomics pathway findings reflected physiology *in vitro*, studies were performed using the L6 rat skeletal muscle cell culture model. The integrity of the model system was evaluated by standard cell viability and cell death measurements post treatment with both sulfonyl isoxazoline compounds. Skeletal muscle toxicity of the sulfonyl isoxazoline compounds (to maximum solubility) was investigated in L6 cells over 24 h. As shown in Fig. 2, with increasing concentration of compounds 177 and 197 decreased cell viability and ATP content was observed in L6 cells. A time course with the highest concentrations of compounds 177 and 197 in L6 cells suggested ATP was significantly depleted after only 2 h (to 67% and 44% of control, respectively), whilst cell viability remained unaffected. Since ATP depletion is an early event in mitochondrial dysfunction, these results support the hypothesis from *in vivo* transcriptomics analysis that the sulfonyl isoxazoline compounds target the mitochondria of skeletal muscle cells as a plausible mechanism of toxicity.

Apoptosis increased in a concentration-dependent manner for compounds 177 and 197 (Fig. 3). Both compounds increased caspase activity in a time and dose-dependent manner (Fig. 3); by 16–24 h, both produced a significant increase in caspase activity at all concentrations investigated.

3.6. Effect of sulfonyl isoxazoline compounds on mitochondrial function

Transcriptomics analysis identified pathways relating to mitochondrial dysfunction as amongst the most affected following treatment with compounds 177 and 197 *in vivo*. Moreover, the time course for cell viability and ATP depletion in L6 cells implicated mitochondrial

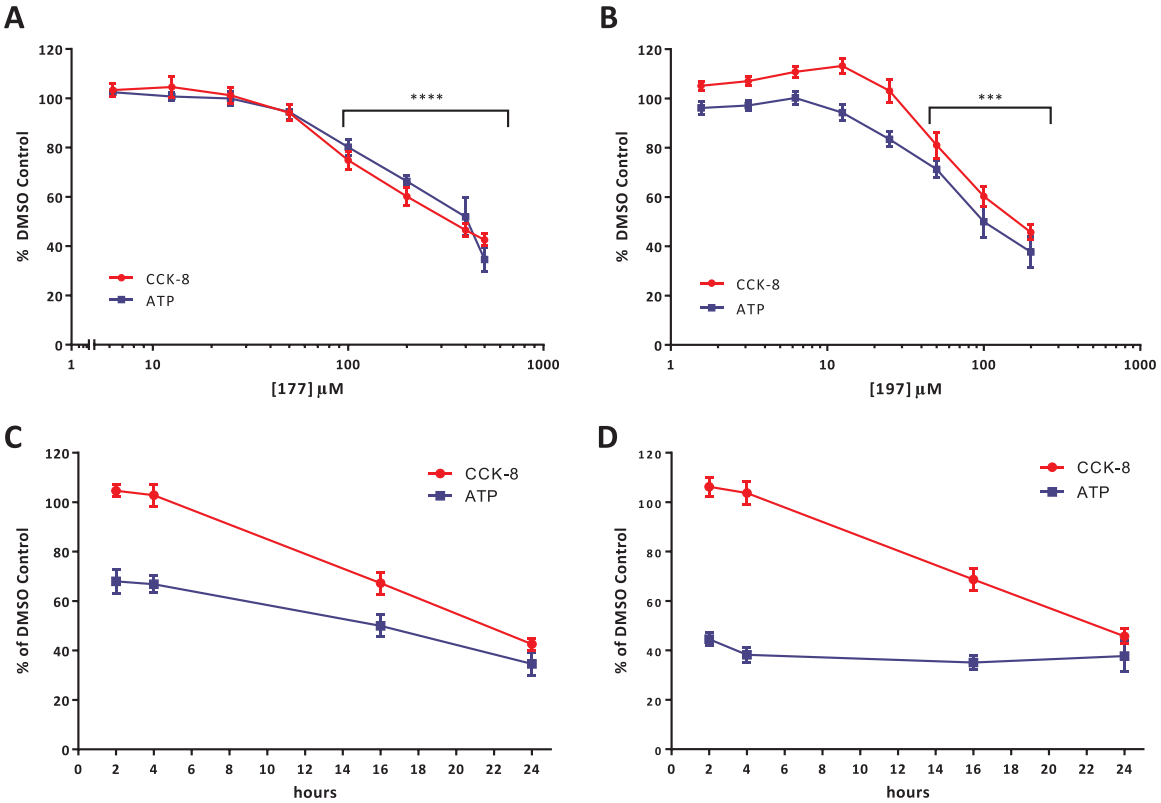

Fig. 2. Cytotoxicity of compounds 177 and 197 in L6 cells. L6 cells were treated with compounds 177 and 197 for 24 h and ATP content and cell viability (CCK-8) were assessed. A and B represent concentration responses in L6 cells for compounds 177 and 197, respectively. Results represent the mean ± SEM; n = 5–7 (***P < 0.001, ****P < 0.0001 Control *vs.* Treated). L6 cells were treated with (C) 500 µM 177, (D) 200 µM 197 for 2, 4, 16 and 24 h and cell viability (CCK-8) (red) and ATP (blue) content were assessed. Results represent the mean ± SEM; n = 3 (*P < 0.05, ****P < 0.0001 CCK-8 *vs.* ATP).

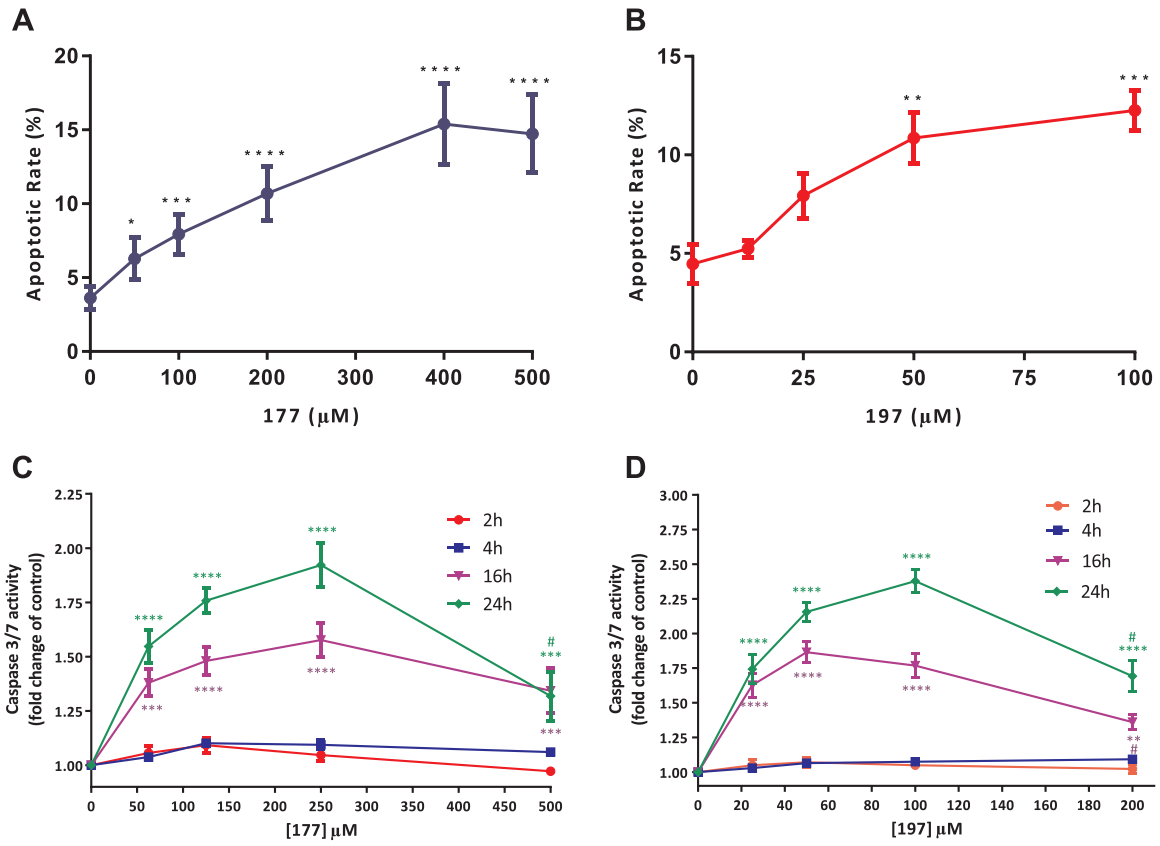

Fig. 3. Sulfonyl isoxazoline compound induced apoptosis in L6 cells. Cells were treated with a range of 177 and 197 concentrations, along with staurosporine and H_2O_2 positive controls, for 24 h. Annexin V/PI staining was used to assess apoptosis using FACS analysis. The apoptotic rate for 177 (A) and 197 (B) was calculated as the percentage of cells in early (annexin V positive) and late apoptosis (annexin V positive and PI positive). Under these conditions, the apoptotic rates for staurosporine (250 nM) and H_2O_2 (2 mM) were 54% and 98%, respectively. Bars represent the mean +SEM; n = 3 (*P < 0.05, **P < 0.01, ***P < 0.001, ****P < 0.0001 control *vs.* treated). Time course of caspase-3/7 activity following treatment of L6 cells treated with a dose range of compound 197 (C) and compound 177 (D). Results represent mean ± SEM; n = 3 (***P < 0.001, ****P < 0.0001 control *vs.* treated; 197 #P < 0.01 200 µM *vs.* 100 µM; 177 #P < 0.01 500 µM *vs.* 250 µM).

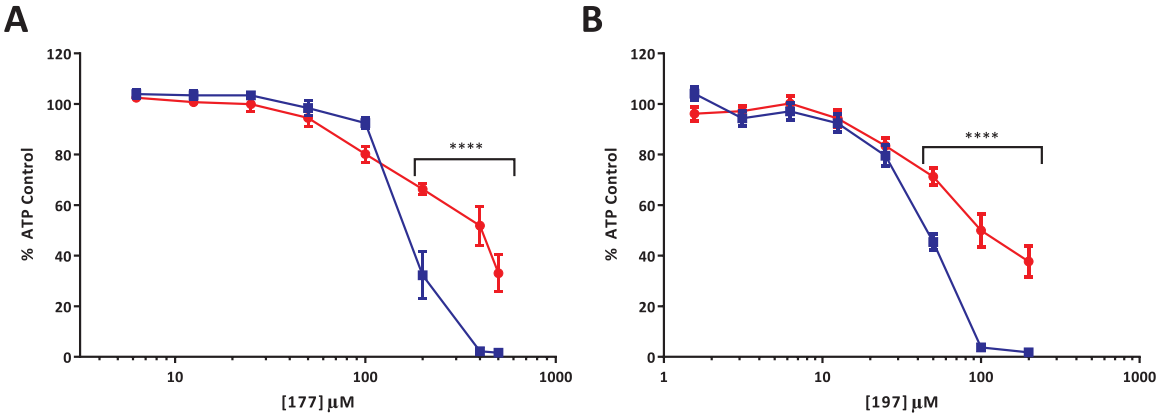

Fig. 4. Effect of sulfonyl isoxazoline compounds on ATP levels in L6 cells. Concentration responses for high-glucose-grown (25 mM) (red) and galactose-grown (10 mM) (blue) L6 cells treated with **(A)** 177 **(B)** 197. After 24 h treatment the ATP content was assessed. Data are mean ± SEM; n = 3 (****P < 0.0001 glucose *vs.* galactose).

perturbation as a possible early event in the toxicity of these compounds (Fig. 2C,D).

Previously, we showed that L6 cells, like HepG2 and H9c2 cells, are able to adapt to growth in galactose media and are consequently more susceptible to mitochondrial toxicants [1]. This model was used to investigate possible effects of compounds 177 and 197 on mitochondrial function. The principle of the model is that cells cultured in galactose are unable to generate sufficient ATP from glycolysis and so are forced to rely on mitochondrial oxidative phosphorylation for ATP generation and consequently are more sensitive to mitochondrial perturbation than cells grown in glucose. L6 cells were cultured in glucose and galactose media for a minimum of 7 days prior to treatment with a range of concentrations of compounds 177 and 197 for 24 h. Cells cultured in galactose media were significantly more sensitive to compounds 177 (≥200 µM) and 197 (≥50 µM) than cells cultured in glucose (Fig. 4). The IC50 ratios demonstrated that L6 cells grown in galactose were at least 2-fold more sensitive to compounds 177 and 197 than glucose grown cells (Table 4). These data demonstrate that the mitochondria are a plausible mode of toxicity for these compounds and that *in vivo* transcriptomics translated into *in vitro* mitochondrial toxicity. Since

Table 4
IC50 values of compounds 177 and 197 in L6 cells cultured in glucose and galactose media.

	IC50μM		IC50 Ratio
Compound	Glucose	Galactose	Glucose / Galactose
177	350.8	170.1	2.1
197	112.1	43.5	2.6

A nonlinear regression was fitted to the concentration response curves from Fig. 3. Maximum (DMSO control = 100% ATP) and minimum values (total cell kill = 0%) were defined.

changes in *in vivo* gene expression strongly implicated 'oxidative stress' and 'energy metabolism', the mechanism of mitochondria toxicity was further investigated.

3.7. Effect of compounds 177 and 197 on mitochondrial bioenergetics in L6 cells

To assess the effects of compounds on L6 cell mitochondrial bioenergetics, the rates of glycolysis and mitochondrial respiration (OXPHOS) were determined by measuring proton release (extracellular acidification rate (ECAR)) and oxygen consumption rate (OCR) using extracellular flux (XF) analysis [28]. L6 cells cultured in glucose and galactose media for a minimum of 7 days were treated with a range of concentrations of sulfonyl isoxazoline compound for 4 h. Baseline measurements of OCR and ECAR were then made and mitochondrial function was assessed using a mitochondrial stress test, which involved the sequential addition of oligomycin, carbonyl cyanide-4-(trifluoromethoxy)phenylhydrazone (FCCP) and AMA. Since the maximum DMSO concentration used for the extracellular flux analysis was limited to 0.2% (v/v) DMSO, the maximum concentration achieved with the compounds was 200 μM. Given that compound 177 was less potent than compound 197, a full concentration-response, after 4 h exposure of L6 cells, was only possible for 197.

The individual mitochondrial function parameters were derived as detailed in [1] and the AUC was calculated for each parameter (Fig. 5). Compound 197 concentration-dependently decreased the OCR in L6 cultured in glucose and galactose containing media (Fig. 5A and B).

In both glucose- and galactose-grown L6 cells, proton leak, ATP-linked OCR, maximal OCR and non-mitochondrial OCR were reduced in a concentration-dependent fashion following compound 197 treatment (Fig. 5E/F). There was no significant difference in the coupling efficiency between DMSO control and treated cells cultured in glucose or galactose media (Fig. 5G). This means there was a proportional decrease in proton leak and ATP-linked OCR following compound 197 treatment of glucose and galactose grown L6 cells.

There was no significant change in the ECAR activity of galactose grown cells following compound 197 treatment (Fig. 5D/H). In contrast, as expected for cells with induced mitochondrial dysfunction, there was a concentration-dependent increase in ECAR activity in glucose cultured cells (Fig. 5C/H). At all concentrations of 197, the activity of ECAR was significantly higher in glucose than in galactose cultured cells (Fig. 5H).

3.8. Generation of cytosolic and mitochondrial superoxide by sulfonyl isoxazoline compounds in L6 cells

Based on the *in vivo* toxicogenomic analysis, oxidative stress was hypothesised to play an important role in mediating the toxicological effects of compounds 177 and 197. Therefore, the ability of these compounds to induce cytosolic and mitochondrial derived superoxide generation was assessed using the fluoroprobes DHE and MitoSox, respectively. The generation of superoxide was assessed after 1 and 24 h treatment with compounds 177, 197 and using AMA as a positive control. Importantly, the fluorescence intensities of the sulfonyl isoxazoline compounds were similar to the fluorescence of control cells not loaded with either fluoroprobe, thereby confirming that the compounds did not autofluoresce in a way that interfered with DHE and MitoSox fluorescence (Fig. 6A).

After 1 h treatment, the highest concentration of compounds 177 (400 μM) and 197 (100 μM) slightly increased the DHE intensity, by 1.4 and 1.6 fold, respectively (Fig. 6A-C). Following 24 h treatment with compounds 177 and 197 there was a considerable increase in MitoSox intensity compared with 1 h, but only a very small increase in DHE intensity (Fig. 6D). Taken together, these results indicate that compounds 177 and 197 increase cytosolic and mitochondrial derived superoxide generation with increasing concentration and increasing exposure time. However, the fold increase in cytosolic derived superoxide was lower than that of mitochondrial derived superoxide after both 1 and 24 h, suggesting that the mitochondria were the primary source of superoxide following sulfonyl isoxazoline treatment.

3.9. Protection of sulfonyl isoxazoline compound-induced mitochondrial superoxide generation and ATP depletion by N-acetylcysteine

NAC was used to confirm that 177 and 197-induced increase in MitoSox intensity was the result of mitochondrial oxidant generation. In addition, NAC was used to assess the involvement of mitochondrial superoxide in ATP-depletion by the compounds. NAC acts as a glutathione precursor and possibly as a direct scavenger of oxidant species [29]. A combination of pre-treatment with NAC for 3 h followed by co-treatment with compounds 177 and 197 for 24 h was used.

NAC (2.5 mM) decreased the mean MitoSox fluorescence intensity induced by compound 177 (Fig. 7A) and compound 197 (Fig. 7B). Quantitative measurements demonstrated that NAC inhibited the generation of MitoSox fluorescence intensity by 177 and 197 (Fig. 7C,D). NAC alone had no effect on MitoSox fluorescence intensity, thereby confirming that the NAC concentrations used were sub-cytotoxic. The ability of NAC to reduce the increase in MitoSox intensity was further confirmation that the compounds 177 and 197 increased mitochondrial superoxide generation.

To assess if mitochondrial oxidant production played an important role in ATP depletion by the two compounds, the effect of NAC on the ATP content of treated L6 cells was determined. A concentration response with NAC alone showed that at concentrations up to 2.5 mM, NAC did not significantly affect ATP levels (data not shown). NAC inhibited sulfonyl isoxazoline compound-induced ATP depletion with increasing concentration and at 2.5 mM, NAC was able to completely inhibit the ATP depletion induced by 50–200 μM compound 177 (Fig. 7E). Treatment with compound 197 showed a similar effect, with 2.5 mM NAC able to maintain ATP levels close to control for cells exposed to 25–100 μM compound 197 (Fig. 7F).

4. Discussion

This study investigated *in vivo* skeletal muscle toxicity at the transcriptome level and explored the translation of perturbed physiological pathways to an *in vitro* cell model. Given the array of *in vivo* findings associated with the novel sulfonyl isoxazoline compounds, the transcriptome data from various tissues were analysed without any predetermined bias (full transcriptome data from all tissues not detailed in this publication). A major advantage of using the novel sulfonyl isoxazoline compounds, as opposed to a well characterised reference skeletal muscle toxicant, for comparison of *in vitro* and *in vivo* responses, was that it avoided any potential bias when selecting toxicity pathways from *in vivo*.

Previous studies have compared the transcriptome responses in *in vivo* and *in vitro* models. These studies identified that the comparison at the level of individual gene expression proved challenging, given that individual genes do not provide information on mechanisms of toxicity

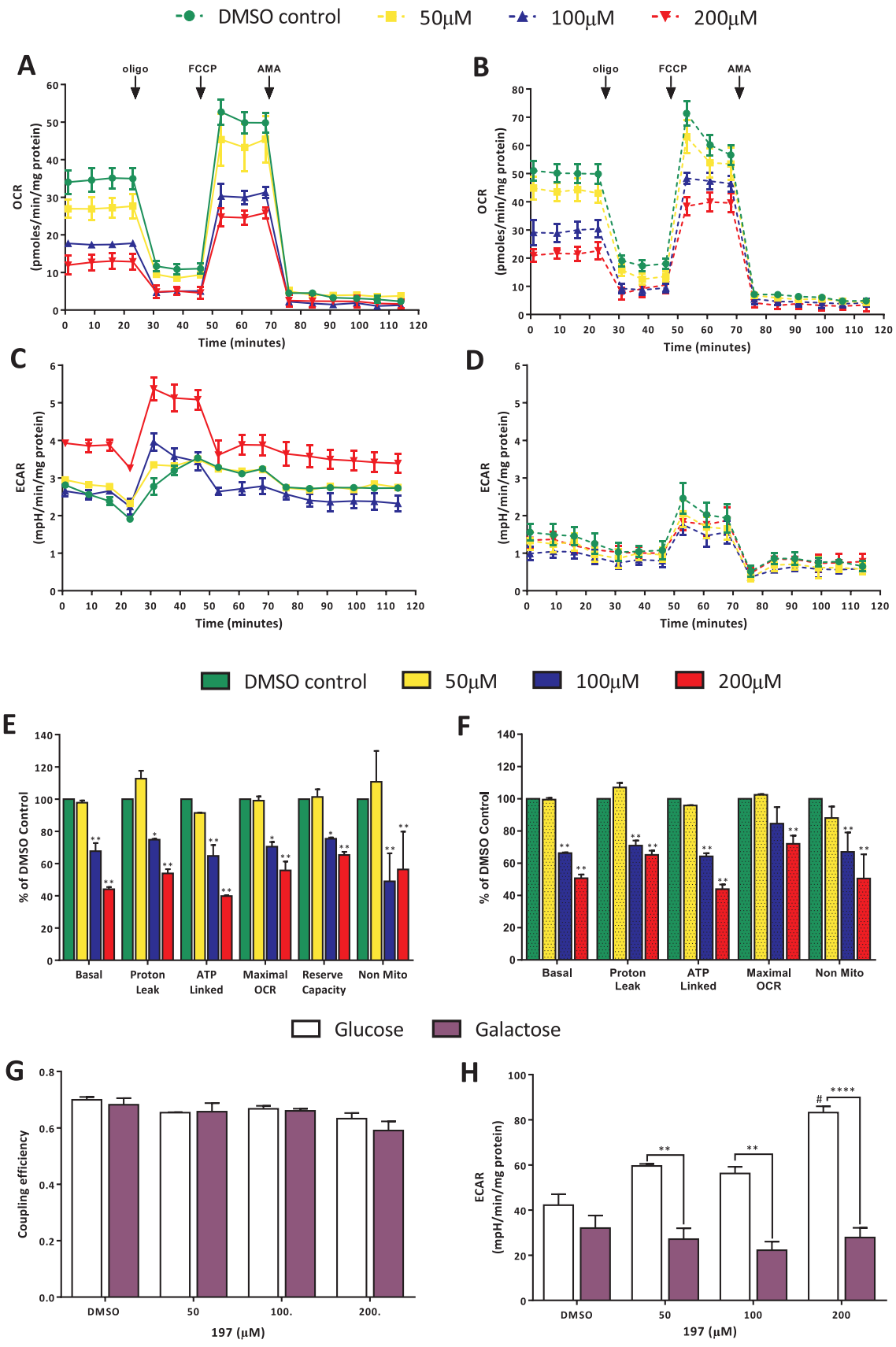

(caption on next page)

Fig. 5. (A-D) Effect of compound 197 on mitochondrial bioenergetics in L6 cells. L6 cells were cultured in glucose or galactose media for a minimum of 7 days. Cells were treated with 50 μM (yellow), 100 μM (blue) and 200 μM (red) of 197 for 4 h. Basal OCR and ECAR of glucose (A and C) and galactose (B and D) cells were then measured followed by sequential injection of oligomycin (800 nM), FCCP (800 nM) and AMA (200 nM) at the times indicated. Results represent mean ± SEM; n = 3. The mitochondrial function parameters of glucose (E) and galactose (F) cultured L6 cells were derived from A and B as described previously [1]. Results represent mean + SEM; n = 3 (*P < 0.05, **P < 0.01 control *vs.* treated). (G) Coupling efficiency was calculated by dividing ATP-linked OCR by basal OCR to determine fraction of basal OCR used for ATP synthesis in glucose and galactose cells following compound 197 treatment. Results represent mean + SEM; n = 3. (H) AUC for basal ECAR activity was calculated from Fig. 4C and D in glucose and galactose cells following 197 treatment. Results represent mean +SEM; n = 3 (**P < 0.01, ****P < 0.0001 glucose *vs.* galactose; #P < 0.05 control *vs.* treated).

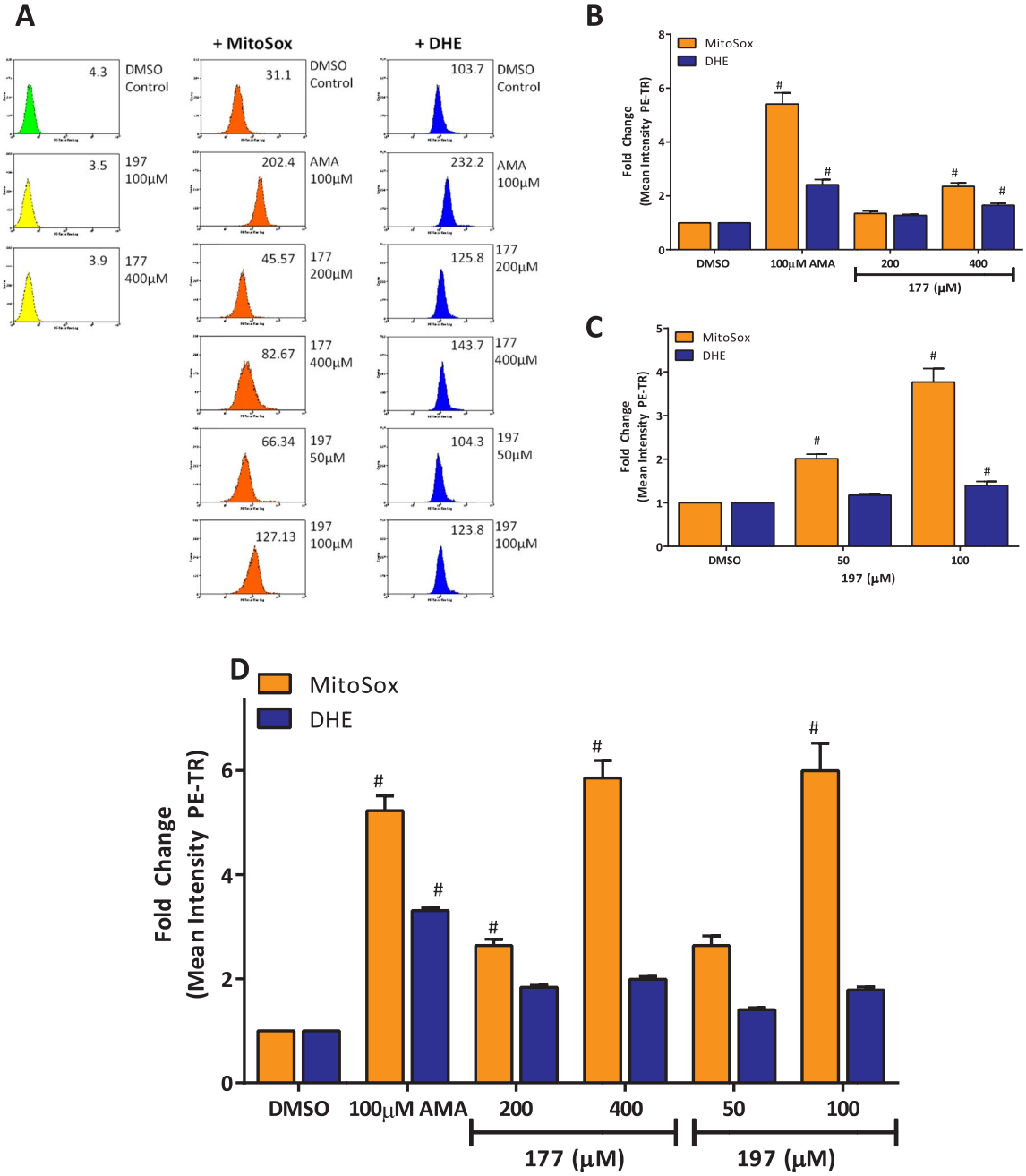

Fig. 6. (A-D) Compounds 177 and 197 increased cystolic and mitochondrial superoxide formation in L6 cells. Cells were treated with 177, 197 and AMA for 1 and 24 h and superoxide production assessed with MitoSox and DHE using flow cytometry. (A) Representative histograms demonstrating dose-dependent increase in the mean fluorescence intensity (PE-Texas Red(PE-TR)) of oxidized DHE (blue) and MitoSox (orange) following 1 h AMA, 177 and 197 treatment as indicated. (B) and (C) Quantitative data expressing increase in mean fluorescence intensity of oxidized DHE and MitoSox following 1 h AMA, 177 (B) and 197 (C) treatment. (D) Quantitative data expressing increase in mean fluorescent intensity of oxidized DHE and MitoSox following 24 h treatment with AMA and compounds 177 and 197. Results represent the mean +SEM; n = 3 (#P < 0.05 treated *vs.* respective fluoroprobe control).

[6–8]. Moreover, the temporal and transient nature of gene expression makes accurate gene comparisons of subtly expressed genes difficult [30]. Instead, these studies suggest it is of more relevance to investigate the biological pathways these genes contribute to. This therefore enabled us to explore the translation of toxicity mechanisms identified *in vivo* in an *in vitro* skeletal muscle model using high-throughput and sensitive biochemical endpoints.

In this study, processes that were perturbed *in vivo* included mitochondrial dysfunction (*e.g. OXPHOS* and *mitochondrial inner membrane*), oxidative stress, energy metabolism, cell death, protein

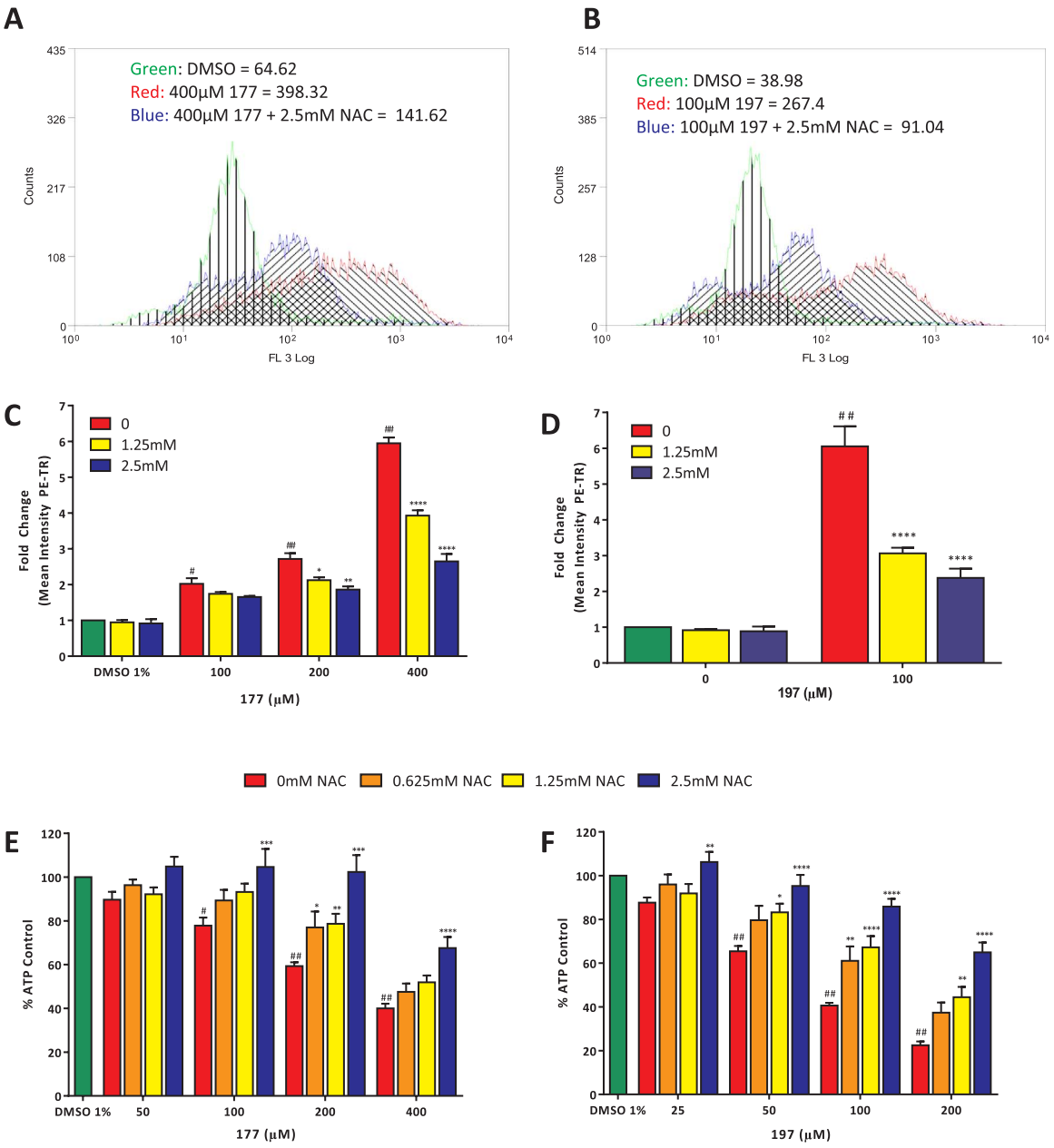

Fig. 7. Inhibition of compound 177 and 197-induced mitochondrial superoxide and ATP depletion by NAC in L6 cells. Cells were pre-treated for 3 h with NAC and then co-treated with NAC and compounds 177 or 197 for a further 24 h. Following treatment, mitochondrial superoxide generation (A-D) was determined with MitoSox using flow cytometry and ATP content (E, F) was measured. (A, B) Representative histograms demonstrating a decrease in MitoSox mean fluorescence intensity by due to compounds compound 177 (A) and compound 197 (B) following pre-treatment with NAC. (C, D) Concentration-dependent inhibition in MitoSox mean fluorescent intensity by NAC for (C) compound 177 and (D) compound 197. (E, F) Concentration-dependent reduction in ATP depletion by NAC for compounds 177 and 197. Bars represent mean +SEM; n = 3 (#P < 0.05, ##P < 0.0001 control *vs.* treated; *P < 0.05, **P < 0.01, ***P < 0.001, ****P < 0.0001 treated *vs.* treated + NAC).

regulation and cell cycle. Mitochondrial dysfunction was further explored *in vitro* as a plausible mechanism of toxicity relating to both of the sulfonyl isoxazoline compounds. The L6 skeletal muscle model was utilised as a sensitive system to explore the translation of *in vivo* transcriptomic data to *in vitro* physiological changes. Both compounds depleted ATP levels after only 2 h in L6 cells, while cell viability remained unaffected, which is indicative of early deleterious changes in mitochondrial function. In addition, the L6 galactose media model [1] demonstrated that mitochondria were a primary target for sulfonyl isoxazoline compound toxicity. Further experiments carried out with the XF analyser showed that compound 197 decreased OXPHOS by ~50% after 4 h, and concomitantly up regulated glycolysis. This is characteristic of mitochondrial toxicity and has been observed with other compounds [31,32]. Analysis of mitochondrial function suggested that compound 197 did not inhibit ATPase or uncouple the mitochondrial membrane potential to induce toxicity. Overall, the XF analyser data provided further evidence that compound 197 had a deleterious effect on the mitochondria and energy metabolism, although it did not elucidate a specific mechanism of toxicity. However, the *in vivo* transcriptomics highlighted oxidative stress as amongst the most significantly enriched biological process in response to compounds 177 and 197 in all tissues. Notably, the Nrf2 pathway, which is regarded as the most important in the cell to protect against xenobiotic and radiation induced electrophilic and oxidative stress [33,34] was significantly enriched by both compounds. The subsequent *in vitro* experiments provided evidence for oxidative stress as the key mechanism inducing mitochondrial dysfunction, with compounds 177 and 197 inducing significant amounts of mitochondrial-derived $O_2^{\bullet-}$. Significantly, NAC

reduced superoxide generation and prevented ATP depletion induced by compounds 177 and 197, suggesting that ATP depletion was the result of mitochondrial $O_2^{\bullet-}$ production. These results imply that the sulfonyl isoxazoline compounds did not inhibit the mitochondrial ETC to induce $O_2^{\bullet-}$, otherwise ATP would have depleted regardless of the antioxidant effect of NAC [35]. Therefore, it can be hypothesised that perhaps the sulfonyl isoxazoline compounds redox cycle to generate $O_2^{\bullet-}$, although this would require further investigation. One limitation of this study is the application of DHE and MitoSOX in flow cytometry to assess $O_2^{\bullet-}$ production in cells. These probes react with oxidants to produce two main fluorescent products, ethidium (mitoethidium) and 2-hydroxyethidium (2-hydroxymitoethidium). However, only the 2-hydroxylated products are somewhat specific for $O_2^{\bullet-}$ and chromatographic separation is required to discriminate between the two products [36]. Further investigations will therefore be required to establish whether or not the sulfonyl isoxazoline compounds generate $O_2^{\bullet-}$ and if so, by what mechanism.

It should be noted that the time course and concentrations used in this study were a reflection of experimental expediency and system tolerability, rather than an actual reflection of *in vivo* exposure. While the parameters used in this study were sufficient to study the mechanistic effects of the sulfonyl isoxazoline compounds, some xenobiotics may need extended exposure or additional metabolic processing. The potency differences of the sulfonyl isoxazoline compounds were difficult to gauge in these limited experiments, whilst compound 197 appeared more toxic than compound 177 across all *in vitro* endpoints studied, the latter proved less well tolerated *in vivo*. These differences may be related to differences in uptake and metabolic processes; however this indicates that refinements (such as co-culture with a microfluidic system) to the *in vitro* system may be required if this model were to be used to rank the potency of toxicity of a range of compounds. Nevertheless, these results do show that the L6 cell line expresses the relevant toxicity pathways to potentially predict *in vivo* outcome. The galactose media model also allows the required sensitivity to study mitochondrial processes.

In conclusion, pathway analysis of *in vivo* transcriptomics data provides a useful guide to further explore physiological changes within *in vitro* surrogate model systems. In addition, we confirm that the L6 galactose model provides an appropriate and sensitive platform to study mitochondrial dysfunction associated with *in vivo* skeletal muscle toxicity.

Funding

WD was in receipt of a Biotechnology and Biological Sciences Research Council (BBSRC, U.K.) (BB/H530962/1) Industrial CASE Studentship in association with Syngenta.

Acknowledgments

We would like to thank Dr Nicholas Sylvius and Mrs Reshma Vaghela of the Genomics Core Facility, University of Leicester for help with performing transcriptomics and analysis of this data.

Appendix A. Supplementary material

Supplementary data associated with this article can be found in the online version at http://dx.doi.org/10.1016/j.redox.2017.09.006.

References

[1] W. Dott, P. Mistry, J. Wright, K. Cain, K.E. Herbert, Modulation of mitochondrial bioenergetics in a skeletal muscle cell line model of mitochondrial toxicity, Redox Biol. 2 (2014) 224–233.
[2] L.D. Marroquin, J. Hynes, J.A. Dykens, J.D. Jamieson, Y. Will, Circumventing the Crabtree effect: replacing media glucose with galactose increases susceptibility of HepG2 cells to mitochondrial toxicants, Toxicol. Sci. 97 (2007) 539–547.
[3] J.A. Dykens, L.D. Marroquin, Y. Will, Strategies to reduce late-stage drug attrition due to mitochondrial toxicity, Expert Rev. Mol. Diagn. 7 (2007) 161–175.
[4] E.A. Blomme, Y. Yang, J.F. Waring, Use of toxicogenomics to understand mechanisms of drug-induced hepatotoxicity during drug discovery and development, Toxicol. Lett. 186 (2009) 22–31.
[5] C.A. Afshari, H.K. Hamadeh, P.R. Bushel, The evolution of bioinformatics in toxicology: advancing toxicogenomics, Toxicol. Sci. 120 (Suppl. 1) (2011) S225–S237.
[6] A.S. Kienhuis, H.M. Wortelboer, J.C. Hoflack, E.J. Moonen, J.C. Kleinjans, B. van Ommen, J.H. van Delft, R.H. Stierum, Comparison of coumarin-induced toxicity between sandwich-cultured primary rat hepatocytes and rats in vivo: a toxicogenomics approach, Drug Metab. Dispos. 34 (2006) 2083–2090.
[7] E. Dere, D.R. Boverhof, L.D. Burgoon, T.R. Zacharewski, In vivo-in vitro toxicogenomic comparison of TCDD-elicited gene expression in Hepa1c1c7 mouse hepatoma cells and C57BL/6 hepatic tissue, BMC Genom. 7 (2006) 80.
[8] F. Boess, E. Durr, N. Schaub, M. Haiker, S. Albertini, L. Suter, An in vitro study on 5-HT6 receptor antagonist induced hepatotoxicity based on biochemical assays and toxicogenomics, Toxicol. Vitr. 21 (2007) 1276–1286.
[9] Y. Jo, J.H. Oh, S. Yoon, H. Bae, M. Hong, M. Shin, Y. Kim, The comparative analysis of in vivo and in vitro transcriptome data based on systems biology, Biochip J. 6 (2012) 280.
[10] F. Charaten, Bayer decides to withdraw cholesterol drug, Br. Med. J. 323 (2001) 359.
[11] W. Tong, X. Cao, S. Harris, H. Sun, H. Fang, J. Fuscoe, A. Harris, H. Hong, Q. Xie, R. Perkins, L. Shi, D. Casciano, ArrayTrack–supporting toxicogenomic research at the U.S. food and drug administration National Center for Toxicological Research, Environ. Health Perspect. 111 (2003) 1819–1826.
[12] M. Barnes, J. Freudenberg, S. Thompson, B. Aronow, P. Pavlidis, Experimental comparison and cross-validation of the Affymetrix and Illumina gene expression analysis platforms, Nucleic Acids Res. 33 (2005) 5914–5923.
[13] M.J. Dunning, N.L. Barbosa-Morais, A.G. Lynch, S. Tavare, M.E. Ritchie, Statistical issues in the analysis of Illumina data, BMC Bioinforma. 9 (2008) 85–2105-9-85.
[14] R. Edgar, M. Domrachev, A.E. Lash, Gene expression omnibus: ncbi gene expression and hybridization array data repository, Nucleic Acids Res. 30 (2002) 207–210.
[15] Y. Benjamini, Y. Hochberg, Controlling the false discovery rate: a practical and powerful approach to multiple testing, J. R. Stat. Soc. 57 (1995) 289.
[16] A. Subramanian, P. Tamayo, V.K. Mootha, S. Mukherjee, B.L. Ebert, M.A. Gillette, A. Paulovich, S.L. Pomeroy, T.R. Golub, E.S. Lander, J.P. Mesirov, Gene set enrichment analysis: a knowledge-based approach for interpreting genome-wide expression profiles, PNAS 102 (2005) 15545–15550.
[17] D.B. Allison, X. Cui, G.P. Page, M. Sabripour, Microarray data analysis: from disarray to consolidation and consensus, Nat. Rev. Genet. 7 (2006) 55–65.
[18] V.V. Smeianov, P. Wechter, J.R. Broadbent, J.E. Hughes, B.T. Rodriguez, T.K. Christensen, Y. Ardo, J.L. Steele, Comparative high-density microarray analysis of gene expression during growth of Lactobacillus helveticus in milk versus rich culture medium, Appl. Environ. Microbiol. 73 (2007) 2661–2672.
[19] N. Juretic, U. Urzua, D.J. Munroe, E. Jaimovich, N. Riveros, Differential gene expression in skeletal muscle cells after membrane depolarization, J. Cell. Physiol. 210 (2007) 819–830.
[20] W. Huang da, B.T. Sherman, R.A. Lempicki, Bioinformatics enrichment tools: paths toward the comprehensive functional analysis of large gene lists, Nucleic Acids Res. 37 (2009) 1–13.
[21] B.G. Hill, G.A. Benavides, J.R. Lancaster, S. Ballinger, L. Dell'Italia, J. Zhang, V.M. Darley-Usmar, Integration of cellular bioenergetics with mitochondrial quality control and autophagy, Biol. Chem. 393 (2012) 1485–1512.
[22] W. Dott, Development and Validation of an in Vitro Model to Explore Mechanisms of Skeletal Muscle Toxicity (Ph.D. Thesis), University of Leicester, 2014 (Available at: ⟨http://hdl.handle.net/2381/28597⟩).
[23] A.B. Singh, R.S. Guleria, I.T. Nizamutdinova, K.M. Baker, J. Pan, High glucose-induced repression of RAR/RXR in cardiomyocytes is mediated through oxidative stress/JNK signalling, J. Cell Physiol. 227 (2012) 2632–2644.
[24] M.H. Yan, X. Wang, X. Zhu, Mitochondrial defects and oxidative stress in Alzheimer disease and Parkinson disease, Free Radic. Biol. Med. 62 (2013) 90–101.
[25] C.M. Chen, Mitochondrial dysfunction, metabolic deficits, and increased oxidative stress in Huntington's disease, Chang Gung Med. J. 34 (2011) 135–152.
[26] R. Doidge, S. Mittal, A. Aslam, G.S. Winkler, The anti-proliferative activity of BTG/TOB proteins is mediated via the Caf1a (CNOT7) and Caf1b (CNOT8) deadenylase subunits of the Ccr4-not complex, PLoS One 7 (2012) e51331.
[27] R.J. Dowling, I. Topisirovic, B.D. Fonseca, N. Sonenberg, Dissecting the role of mTOR: lessons from mTOR inhibitors, Biochim. Biophys. Acta 1804 (2010) 433–439.
[28] D.A. Ferrick, A. Neilson, C. Beeson, Advances in measuring cellular bioenergetics using extracellular flux, Drug Discov. Today 13 (2008) 268–274.
[29] A. Gillissen, D. Nowak, Characterization of N-acetylcysteine and ambroxol in antioxidant therapy, Respir. Med. 92 (1998) 609–623.
[30] G. Chechik, D. Koller, Timing of gene expression responses to environmental changes, J. Comput. Biol. 16 (2009) 279–290.
[31] V.M. Gohil, S.A. Sheth, R. Nilsson, A.P. Wojtovich, J.H. Lee, F. Perocchi, W. Chen, C.B. Clish, C. Ayata, P.S. Brookes, V.K. Mootha, Discovery and therapeutic potential of drugs that shift energy metabolism from mitochondrial respiration to glycolysis, Nat. Biotechnol. 28 (2010) 249.
[32] C. Reily, T. Mitchell, B.K. Chacko, G. Benavides, M.P. Murphy, V. Darley-Usmar, Mitochondrially targeted compounds and their impact on cellular bioenergetics, Redox Biol. 1 (2013) 86–93.
[33] A.K. Jaiswal, *Nrf2 signal*ing in coordinated activation of antioxidant gene expression, Free Radic. Biol. Med. 36 (2004) 1199–1207.
[34] I.M. Copple, C.E. Goldring, N.R. Kitteringham, B.K. Park, The Nrf2-Keap1 defence

pathway: role in protection against drug-induced toxicity, Toxicology 246 (2008) 24–33.
[35] M. Watabe, T. Nakaki, ATP depletion does not account for apoptosis induced by inhibition of mitochondrial electron transport chain in human dopaminergic cells, Neuropharmacology 52 (2007) 536–541.
[36] B. Kalyanaraman, V. Darley-Usmar, K.J. Davies, P.A. Dennery, H.J. Forman, M.B. Grisham, G.E. Mann, K. Moore, L.J. Roberts 2nd, H. Ischiropoulos, Measuring reactive oxygen and nitrogen species with fluorescent probes: challenges and limitations, Free Radic. Biol. Med. 52 (2012) 1–6.